February 2008

# A Thermodynamic Investigation of the Redox Properties of Ceria-Titania Mixed Oxides

Gong Zhou
*University of Pennsylvania*

Jonathan Hanson
*Brookhaven National Laboratory*

Raymond J. Gorte
*University of Pennsylvania*, gorte@seas.upenn.edu



Postprint version. Published in *Applied Catalysis A General*, Volume 235, Issue 2, February 2008, pages 153-158.
Publisher URL: http://dx.doi.org/10.1016/j.apcata.2007.11.011

# A Thermodynamic Investigation of the Redox Properties of Ceria-Titania Mixed Oxides


## Abstract

Ceria-titania solutions with compositions of $Ce_{0.9}Ti_{0.1}O_2$ and $Ce_{0.8}Ti_{0.2}O_2$ were prepared by the citric-acid (Pechini) method and characterized using x-ray diffraction (XRD) for structure, coulometric titration for redox thermodynamics, and water-gas-shift (WGS) reaction rates. Following calcination at 973 K, XRD suggests that the mixed oxides exist as single-phase, fluorite structures, although there was no significant change in the lattice parameter compared to pure ceria. The mixed oxides are shown to be significantly more reducible than bulk ceria, with enthalpies for reoxidation being approximately -500 kJ/mol O2, compared to -760 kJ/mol $O_2$ for bulk ceria. However, WGS rates over 1-wt% Pd supported on ceria, $Ce_{0.8}Ti_{0.2}O_2$, and $Ce_{0.8}Zr_{0.2}O_2$ were nearly the same. For calcination at 1323 K, the mixed oxides separated into ceria and titania phases, as indicated by both the XRD and thermodynamic results.



## Keywords

ceria-titania, ceria, coulometric titration, thermodynamic properties, oxidation enthalpy, water-gas shift.

## Comments

Postprint version. Published in *Applied Catalysis A General*, Volume 235, Issue 2, February 2008, pages 153-158.
Publisher URL: http://dx.doi.org/10.1016/j.apcata.2007.11.011

# A Thermodynamic Investigation of the Redox Properties of Ceria-Titania Mixed Oxides

Gong Zhou[1], Raymond J. Gorte[1*]
[1]Department of Chemical and Biomolecular Engineering
University of Pennsylvania
Philadelphia, PA 19104, USA

Jonathan Hanson[2]
Chemistry Department, Brookhaven National Laboratory
Upton, NY 11973, USA

## Abstract

Ceria-titania solutions with compositions of $Ce_{0.9}Ti_{0.1}O_2$ and $Ce_{0.8}Ti_{0.2}O_2$ were prepared by the citric-acid (Pechini) method and characterized using x-ray diffraction (XRD) for structure, coulometric titration for redox thermodynamics, and water-gas-shift (WGS) reaction rates. Following calcination at 973 K, XRD suggests that the mixed oxides exist as single-phase, fluorite structures, although there was no significant change in the lattice parameter compared to pure ceria. The mixed oxides are shown to be significantly more reducible than bulk ceria, with enthalpies for reoxidation being approximately -500 kJ/mol $O_2$, compared to -760 kJ/mol $O_2$ for bulk ceria. However, WGS rates over 1-wt% Pd supported on ceria, $Ce_{0.8}Ti_{0.2}O_2$, and $Ce_{0.8}Zr_{0.2}O_2$ were nearly the same. For calcination at 1323 K, the mixed oxides separated into ceria and titania phases, as indicated by both the XRD and thermodynamic results.

**Key Words:** Ceria-titania, Ceria, Coulometric titration, Thermodynamic properties, Oxidation enthalpy, Water-gas shift.

**Introduction**

The ability of cerium dioxide to undergo oxidation and reduction is important for a number of catalytic applications. For example, the redox properties of ceria are certainly important in Oxygen-Storage Capacitance (OSC) for three-way, emissions-control catalysis [1-7] and are likely to be important for water-gas-shift catalysis [8-15], hydrocarbon-reforming catalysis [16,17], and hydrocarbon oxidation in control of diesel emissions [18,19]. Because pure ceria has rather poor thermal stability [20], it is most often used in the form of a mixed oxide. In the case of OSC, the ceria is used as a mixed oxide with zirconia [1-4]. The enhanced reducibility of ceria-zirconia solutions has sometimes been associated with the ability of the solid solutions to maintain high surface areas; however, recent thermodynamic studies in our laboratory have shown that even bulk oxygen is released much more easily in the mixed oxide [21-23]. The enthalpy change for oxidation of reduced oxides was found to be -520 kJ/mol $O_2$ for ceria-zirconia solutions having a range of compositions, compared to an enthalpy change of -760 kJ/mol $O_2$ for pure ceria. Ceria is also commonly doped with +3 rare-earth ions, such as $Sm^{+3}$ and $Gd^{+3}$, since these mixtures are known to exhibit improved ionic conductivity [24]; however, these ions do not appear to influence the thermodynamics of ceria oxidation and reduction in any significant manner [25].

Because enhanced reducibility of ceria is likely to lead to improved catalytic properties for some reactions, there have been many investigations into the properties of other dopants for ceria. One particularly interesting system is that of ceria-titania solutions, with several recent reports indicating that titania doping leads to improved reducibility. First, a study using density functional theory by Andersson, et al compared the reducibility of ceria doped with $Zr^{4+}$, $Hf^{4+}$, $Ti^{4+}$, and $Th^{4+}$ ions and found that ceria doped with $Ti^{4+}$ was the most easily reduced of these materials [26]. $Ti^{4+}$, like $Zr^{4+}$, decreased both the vacancy formation energy and the migration barrier in the ceria. In a study combining both experiments and calculations [27], Dutta, et al also observed enhanced reducibility of ceria-titania solutions, with the mixed oxides undergoing significantly more reduction than either pure titania or ceria in temperature-programmed-reduction (TPR) measurements. These authors also provided spectroscopic evidence for strongly and weakly bound oxygen in the mixed oxides. Finally, Yang, et al reported that ceria-titania catalysts were more active than the pure oxides for aqueous-phase oxidations [28].

Since the reducibility of ceria is affected by many factors [25], we set out to measure the energetics for oxidation of reduced ceria-titania quantitatively on samples where enhanced reducibility could not be due to reduced crystallite sizes or surface-area effects. Our approach was to characterize oxidation and reduction using thermodynamic measurements to determine the enthalpies and entropies for adding oxygen to a partially reduced sample [22,23,25]. Because the equilibrium constant for oxidation of $CeO_{(2-x)}$ is equal to $P(O_2)^{-½}$ (the fugacity of $O_2$), the differential Gibbs Free Energy for oxidation, $\Delta G$, can be determined as a function of x by measuring the oxygen isotherms. The range of $P(O_2)$ values that are of interest for equilibrium measurements is so low as to be experimentally inaccessible, making it necessary to establish oxygen fugacities through equilibrium with $H_2$ oxidation, $H_2 + ½O_2 = H_2O$. Low values for $P(O_2)$ can then be achieved through gas-phase mixtures of $H_2O$ and $H_2$, according to Equation 1.

$$P(O_2)^{½} = K_{equilib}^{-1} * P(H_2O)/P(H_2) \quad (1)$$

Finally, differential oxidation enthalpies, $\Delta H$, can be determined by measuring isotherms at different temperatures, using Equation 2.

$$\Delta H = -R\, \delta \ln(P(O_2))/\delta(1/T)\big|_x \quad (2)$$

What we will show in this paper is that some of the oxygen in titania-doped ceria is very weakly bound, with oxidation enthalpies even lower than that found with ceria-zirconia solutions. Although the ceria-titania solutions are not as stable as ceria-zirconia solutions, they have properties that may make them useful for some catalytic applications.

## Experimental Section

### *Samples*

The $Ce_xTi_{1-x}O_2$ (x=0.9, 0.8, 0.5, and 0.2) mixed oxides were prepared using sol-gel methods similar to those described elsewhere [29]. Stoichiometric amounts of titanium isopropoxide (Aldrich 99.999%) were added dropwise, under vigorous stirring, to an ethanolic solution of $Ce(NO_3)_3 \cdot 6H_2O$ (Aldrich 99.99 %). Ammonium hydroxide was then added dropwise to the solution until a pH of 9 was achieved, resulting in the precipitation of a solid. This precipitate was dried slowly in air at 353 K to remove excess solvent, and then calcined at 973 K in air for 5 h to produce the mixed oxides. Because a preliminary diffraction study of the materials showed that only the $Ce_{0.8}Ti_{0.2}O_2$ and the $Ce_{0.9}Ti_{0.1}O_2$ samples were single phase, these were the only samples that were investigated extensively. Additional calcinations to temperatures

of 1323 K were used to check the phase stability of these two samples and to determine the effect of calcination temperature on the equilibrium properties.

Surface areas were determined by the BET method using $N_2$ or Kr (for samples with very low surface areas) as the adsorbent. The unit-cell parameters, crystallite sizes, and lattice strains were obtained from the powder diffraction patterns collected at beam line X7B of the NSLS at Brookhaven National Laboratory using a Mar345 image plate detector. The data range in these measurements was from 15 to 51° in 2θ (Q~6). The x-ray wavelength (0.9209 nm) and other instrument parameters were determined from a measurement of an $LaB_6$ standard using the program FIT2D [30]. The 2 dimensional patterns were converted to powder patterns with FIT2D. The above parameters were determined by profile fitting using the REFLEX module of the Materials Studio program (Accelrys Software Inc).

For comparison, we also studied $CeO_2$ and $Ce_{0.81}Zr_{0.19}O_2$ samples. The preparation and characterization of the $Ce_{0.81}Zr_{0.19}O_2$ has been discussed extensively elsewhere [21,23]. This material was prepared using the Pechini method and was present as a solid solution. For the present study, it was calcined in air at 723 K and had an initial surface area of 72 $m^2/g$. The $CeO_2$ was prepared by decomposition of cerium nitrate at 723 K and had an initial surface area of 94 $m^2/g$.

***Equilibrium Measurements***

Two techniques were used to measure the equilibrium oxidation isotherms, both of which have been described in detail elsewhere [21-23,25]. The first, flow titration, involved placing between 0.5 and 1.0 g of sample in a quartz-tube flow reactor, then exposing the reduced sample to a flowing mixture of $H_2$ and $H_2O$ at the temperature of interest for 3 h. The water vapor was introduced into the gas stream by passing pure $H_2$ through a temperature-controlled, water bubbler and the $H_2O$ partial pressure was evaluated from the equilibrium vapor pressure. After equilibration of the sample in the $H_2$-$H_2O$ mixture, the reactor was purged with dry He for 0.5 h. Finally, the oxidation state of the sample was determined by measuring the amount of oxygen required for complete re-oxidation. This was accomplished by flowing air (21% $O_2$ and 79% $N_2$) over the sample at a rate of 4.3 ml/min and measuring the composition of the effluent gas from the reactor using a quadrupole mass spectrometer. The $N_2$ signal from the air was used as an internal standard for determining the amount of $O_2$ consumed. That equilibrium was achieved

was shown by the fact that the extent of reduction at a particular $H_2$-$H_2O$ ratio was independent of whether we started with an oxidized or a reduced sample.

Equilibrium information on the samples was also determined using coulometric titration. In this technique, the $P(O_2)$ of the gases over an equilibrated sample are measured electrochemically [22,23,25]. In our apparatus, a 100-mg sample was placed in a sealed container at the temperature of interest and reduced by passing a mixture of 90% He, 10% $H_2$, and 3% $H_2O$ over it. After having been reduced, the sample was sealed in the gas mixture and the equilibrium $P(O_2)$ was measured with an oxygen sensor. The oxygen sensor was essentially a solid oxide fuel cell with a yttria-stabilized zirconia (YSZ) membrane that was part of the container wall. The electrodes for the sensor were made from Ag paste on the reducing side and a composite of YSZ and $La_{0.8}Sr_{0.2}MnO_3$ (LSM) on the air side. In addition to measuring the $P(O_2)$, the sensor was also used to add and remove oxygen from the system through application of a potential across the ion-conducting, YSZ membrane. Because 1 Coulomb is equivalent to 2.6 μmol $O_2$, electrochemical addition of oxygen is very precise. Since $10^{-20}$ atm corresponds to less than one molecule in the apparatus, it should be recognized that the $P(O_2)$ is a fugacity established by equilibrium between $H_2$ and $H_2O$ over most of the $P(O_2)$ range that was investigated.

The criterion we used for establishing equilibrium in coulometric titration was that the potential of the oxygen sensor change by less than 1 mV/h. The time required for achieving equilibrium depended on the temperature and the sample but was typically two days after the addition of oxygen to the sample at temperatures below 873 K in the present experiment. Equilibrium was reached much faster, usually in 4 to 5 h, when the sample temperature was changed without the addition of oxygen. Furthermore, while it was difficult to establish reversibility by electrochemically pumping oxygen from the sample (the pumping rates out of the cell were simply too low), reversibility with temperature changes was checked and achieved in all cases.

***Catalytic Studies***

Because oxygen transfer between ceria and Pd is thought to be important in the water-gas-shift (WGS) reaction over Pd/ceria catalysts [12], we used this reaction for characterizing the effect of titania doping on the catalytic properties of ceria. Pd was added by wet impregnation of $Pd(NH_3)_4(NO_3)_2$ (Aldrich 99.99%) onto the various ceria supports. Rate measurements for the

WGS reaction were performed in a ¼-inch, Pyrex glass, tubular reactor using approximately 0.10 g of catalyst. Water was introduced by saturation of a He carrier gas flowing through a de-ionized water saturator. While the reactor pressure was always atmospheric, the partial pressures of CO, $H_2O$ and He were controlled by adjusting the relative flow rates of each component. All of the reaction measurements in this study were collected with partial pressures for CO and $H_2O$ of 25 torr. For all measurements where rates are reported, the conversions of CO and $H_2O$ were kept well below 10%, so that differential conditions could be assumed. Reaction rates were normalized to the BET surface areas of the samples. The concentration of the effluent from the reactor was determined using an on-line gas chromatograph, SRI8610C, equipped with a Hayesep Q column and a TCD detector

**Results and Discussion**

***Physical Characteristics of the Samples***

The diffraction patterns, measured at Brookhaven NLS, for the ceria-titania samples following calcination at 973 are shown in Fig. 1. The physical characteristics of these samples are reported in Table 1 together with data for pure ceria. After calcination at 973 K, the two ceria-titania samples appeared to be single phase, with a fluorite structure. Both samples had surface areas similar to that reported for pure ceria following calcination at 773 K, although the average crystallite sizes of the ceria-titania samples, estimated from the diffraction line broadening, were significantly lower than that of pure ceria. In agreement with an earlier study [21,23] and unlike the case with ceria-zirconia solutions, the lattice parameters for the ceria-titania oxides are shifted only slightly from that of pure ceria. The small shift in lattice parameters for the ceria-titania solutions can be attributed to the complexity of specific local atomic relaxation around $Ti^{+4}$ ions, which is related to the fact $TiO_2$ prefers the rutile/anatase structures rather than the fluorite structure [31]. Ti incorporation into the fluorite lattice leads to a four-fold tetrahedron-like environment around $Ti^{4+}$ by displacing half of the oxygen ions toward the $Ti^{4+}$ and half away from $Ti^{4+}$. This in turn results in an ordered superstructure, closely related to the original fluorite structure, created by a cubic sub-lattice of $Ti^{4+}$ ions and a separated cubic sub-lattice of displaced oxygen ions [26,32]. These structural differences in the mixed oxides likely explain the relatively high strain reported in Table 1.

After calcination at 1373 K, both ceria-titania samples exhibit weak rutile peaks in the diffraction patterns that indicate separation into ceria and titania phases. There are also

significant increases in the average crystallite sizes and decreases in the specific surface areas. Since the surface areas are more than a factor of 10 smaller than the calculated specific areas of the crystallites, the samples must exist as agglomerates.

***Redox Stability of Ceria-Titania Solutions at 973 K***

In an earlier study of the thermodynamics of surface oxygen in high-surface-area ceria [25], it was observed that the extent of sample reduction and the sample surface area decreased with each redox cycle. For pure ceria, surface area and sample reducibility are related because oxygen at the ceria surface is more weakly bound than oxygen in the bulk [33,34]. For ceria-zirconia solutions, surface-area effects did not appear to play a role in thermodynamic measurements [21], possibly because all of the samples had reasonably low surface areas at the beginning.

With the ceria-titania mixed oxides, it was obviously important to establish that the reducibility of the samples was again unaffected by redox cycling, as in the case of ceria-zirconia solutions, and that any differences in the thermodynamic properties of the mixed oxides were not due to surface-area effects. Therefore, our initial experiments involved flow-titration measurements of the $Ce_{0.8}Ti_{0.2}O_2$ sample in which our sample underwent multiple redox cycles at 973 K over a period of 70 h. The surface area of this sample dropped from 60 $m^2/g$ to 23 $m^2/g$ during the course of these experiments, but the extent of reduction achieved at a given $P(O_2)$ did not change. For example, when the $Ce_{0.8}Ti_{0.2}O_2$ sample was exposed to a gas mixture consisting of 2.8% $H_2O$ and 97.2% $H_2$ at 973 K ($P(O_2) = 1.2x10^{-24}$ atm), the O:M ratio was found to be 1.84 for both the fresh and aged samples. Similar experiments with pure ceria at 873 K, with a 10% $H_2O$-90% $H_2$ mixture ($P(O_2)$ of $1.6x10^{-26}$ atm), caused the surface area to change from 89 $m^2/g$ sample to 25 $m^2/g$, while the equilibrium O:Ce ratio increased from 1.92 for the fresh sample to 1.95 for the aged sample.

***Thermodynamic measurements***

The oxygen isotherms at 973 K for the $CeO_2$, $Ce_{0.9}Ti_{0.1}O_2$ and $Ce_{0.8}Ti_{0.2}O_2$ samples are reported in Fig. 2. Fig. 2 also includes the isotherm measured on $Ce_{0.9}Ti_{0.1}O_2$ after it had been calcined at 1373 K. Data for $TiO_2$ (both rutile and anatase samples were examined) are not shown because the extent of reduction was negligible for both samples (O:M > 1.98 at 973 K and a $P(O_2)$ of $1.2x10^{-24}$ atm). Most of the data on the ceria-containing samples was obtained using coulometric titration. Because coulometric titration does not provide the absolute oxygen

stoichiometries, the O:M stoichiometries were calculated from the amounts of oxygen that were added to the samples, assuming that the samples were completely oxidized (O:M =2) when the $P(O_2)$ reached 0.01 atm. The data for pure $CeO_2$ in this plot agree very well with previous thermodynamic data for ceria, measured using thermogravimetric [35] and flow-titration [21] measurements. Bulk ceria is almost completely oxidized over most of the range of $P(O_2)$ that we studied. The $Ce_{0.9}Ti_{0.1}O_2$ and $Ce_{0.8}Ti_{0.2}O_2$ samples that were calcined at 973 K undergo much deeper reduction than was found for $CeO_2$; and there is again very good agreement between the flow-titration measurements and the coulometric-titration measurements on the $Ce_{0.8}Ti_{0.2}O_2$ sample, providing additional confidence in the techniques.

It is noteworthy that both the $Ce_{0.9}Ti_{0.1}O_2$ and $Ce_{0.8}Ti_{0.2}O_2$ samples that were calcined at 973 K have isotherms with a similar shape and that there is an inflection point in both isotherms at a $P(O_2)$ of approximately $1x10^{-14}$ atm at 973 K. The extent of reduction for the $Ce_{0.8}Ti_{0.2}O_2$ sample at this $P(O_2)$ is clearly higher than that for the $Ce_{0.9}Ti_{0.1}O_2$ sample, with an O:M ratio near 1.90 compared to 1.93. For $Ce_{0.81}Zr_{0.19}O_2$ and $Ce_{0.92}Zr_{0.08}O_2$, plateaus were observed in the isotherms at O:M ratios near 1.90 and 1.95, and it was suggested that these are associated with the formation of $Ce_2Zr_2O_7$-like clusters in the bulk [21,22]. Because the O:M ratios in the ceria-titania samples correspond to stoichiometries that are reasonably close to that found with the ceria-zirconia solutions, we suggest that one may form similar clusters.

The isotherm for the $Ce_{0.9}Ti_{0.1}O_2$ sample calcined at 1373 K is identical to that of pure ceria. The diffraction data in Fig. 1 showed phase separation of ceria and titania after the sample had been heated to this temperature. In agreement with that, the redox properties revert to those of the pure oxides.

The differential enthalpies for reduction of the $Ce_{0.8}Ti_{0.2}O_2$ sample calcined at 973 K were determined from oxygen isotherms measured between 873 and 973 K using Equation 2, and the values are reported together with previous results for $CeO_2$ and $Ce_{0.81}Zr_{0.19}O_2$ in Fig. 3. (In this plot, the extent of sample reduction decreases with increasing O:M ratio.) For $CeO_2$, the oxidation enthalpies that we calculated from the isotherms are very close to the values reported in literature reviews and handbooks, -760 kJ/mol $O_2$ [21,36]. Also in agreement the literature, the oxidation enthalpies for $CeO_2$ are independent of oxygen stoichiometry [21,37]. With $Ce_{0.81}Zr_{0.19}O_2$, the oxidation enthalpies are much lower in magnitude, -520 kJ/mol $O_2$, and are again independent of oxygen stoichiometry so long as the oxygen vacancy concentration is less

than the $Zr^{+4}$ concentration [22]. Based on the observation of steps in the oxygen isotherms at specific stoichiometries [22,23] and the fact that the oxidation enthalpies for ceria-zirconia samples having a wide range of Zr contents are all similar to the heat of oxidation reported for the pyrochlore structure, $Ce_2Zr_2O_7$ [23,38], it has been argued that the redox properties of ceria-zirconia solid solutions result from formation of pyrochlore clusters in the bulk structure, with pairs of $Zr^{+4}$ contributing to two clusters [22,23].

The redox behavior of $Ce_{0.8}Ti_{0.2}O_2$ is somewhat different from that of $CeO_2$ or $Ce_{0.81}Zr_{0.19}O_2$ in that the oxidation enthalpies are a strong function of oxygen stoichiometry. For very low extents of reduction, O:M ratios above 1.95, $-\Delta H$ is only 400 kJ/mol $O_2$. This low value for $-\Delta H$ is consistent with initial observations that we made using flow titration, where we observed that simply heating the $Ce_{0.8}Ti_{0.2}O_2$ sample in flowing He at 973 K caused reduction of the sample to an O:M ratio of 1.95. Based on standard rate pre-exponentials [39], rapid desorption of $O_2$ at 973 K can only occur if $-\Delta H_{adsorption}$ is below 400 kJ/mol $O_2$. By contrast, no reduction was observed for either $CeO_2$ or $Ce_{0.81}Zr_{0.19}O_2$ by heat treatment at 973 K. For high extents of reduction, O:M ratios below 1.85, the enthalpies approach that of $CeO_2$. In the O:M range from 1.9 to 1.95, $-\Delta H$ is similar to that observed with $Ce_{0.81}Zr_{0.19}O_2$.

***WGS Rate Measurements***

In looking for a reaction that would be affected by a lower oxygen binding energy, we focused on the WGS reaction as most likely to be affected by enhanced reducibility of the oxide. For example, in hydrocarbon oxidation, the rate-limiting step likely involves C-C or C-H bond breaking, so that the effect of binding energy is not clear. While the mechanism for the WGS reaction over ceria-supported precious metals remains controversial [40], one proposed mechanism involves oxygen transfer from the ceria to the supported metal. A lower binding energy of the support could therefore result in higher rates.

Fig. 4 shows Arrhenius plots for the WGS reaction in 25 torr of both CO and $H_2O$ for catalysts with 1wt% Pd on $CeO_2$, $Ce_{0.81}Zr_{0.19}O_2$, and $Ce_{0.8}Ti_{0.2}O_2$; BET surface areas for each of the samples and activation energies for the WGS rates are summarized in Table 2. The rates and the activation energy for reaction on the 1wt% $Pd/CeO_2$ sample are in excellent agreement with earlier studies [40]. However, the activities and activation energies for both 1wt% $Pd/Ce_{0.8}Zr_{0.2}O_2$ and 1wt% $Pd/Ce_{0.8}Ti_{0.2}O_2$ were nearly identical to that of 1wt% $Pd/CeO_2$. Since the binding energies for oxygen on surface $CeO_2$ [25],$Ce_{0.81}Zr_{0.19}O_2$ [21-23], and $Ce_{0.8}Ti_{0.2}O_2$ are

all approximately 500 kJ/mol $O_2$, it is possible that differences in the surface properties of these materials are simply not large enough to affect catalytic rates for the WGS reaction and that bulk properties are not relevant in this case.

**Conclusions**

Ceria-titania mixed oxides with compositions of $Ce_{0.8}Ti_{0.2}O_2$ and $Ce_{0.9}Ti_{0.1}O_2$, prepared by the Pechini method and calcined at 973 K, appear to be single phase materials. XRD results are consistent with the materials existing as single phase, fluorite structures. Stronger evidence for the formation of solid solutions comes from thermodynamic studies which show the mixed oxides exhibit significantly lower oxygen binding energies compared to either ceria or titania. However, following calcination at 1323 K, the mixed oxides separate into ceria and titania phases and enhanced reducibility is lost.

**Acknowledgements:**

This work was supported by the Department of Energy, Office of Basic Energy Sciences, Chemical Sciences, Geosciences and Biosciences Division, Grant DE-FG02-85ER13350. The work at Brookhaven National Laboratory was financed by contract DE-AC02-8CH10886 with the U.S. Department of Energy (Division of Chemical Sciences)

**References:**


[1] R.W. Mccabe, J.M. Kisenyi, Chemistry & Industry (1995) 605.
[2] J. Kaspar, P. Fornasiero, N. Hickey, Catalysis Today 77 (2003) 419.
[3] M. Shelef, G.W. Graham, R.W. McCabe, in A. Trovarelli (Editor), Catalysis by Ceria and Related Materials, Imperial College Press; London, 2002.
[4] M. Sugiura, M. Ozawa, A. Suda, T. Suzuki, T. Kanazawa, Bulletin of the Chemical Society of Japan 78 (2005) 752.
[5] T. Masui, T. Ozaki, K.-i. Machida, G.-Y. Adachi, Journal of Alloys and Compounds 303-304 (2000) 49.
[6] M. Ozawa, M. Kimura, A. Isogai, Journal of Alloys and Compounds 193 (1993) 73.
[7] H. Shinjoh, Journal of Alloys and Compounds 408-412 (2006) 1061.
[8] T. Bunluesin, R.J. Gorte, G.W. Graham, Applied Catalysis B-Environmental 15 (1998) 107.
[9] S.Y. Choung, M. Ferrandon, T. Krause, Catalysis Today 99 (2005) 257.
[10] Q. Fu, H. Saltsburg, M. Flytzani-Stephanopoulos, Science 301 (2003) 935.
[11] A.F. Ghenciu, Current Opinion in Solid State & Materials Science 6 (2002) 389.
[12] S. Hilaire, X. Wang, T. Luo, R.J. Gorte, J. Wagner, Applied Catalysis a-General 215 (2001) 271.
[13] G. Jacobs, P.A. Patterson, U.M. Graham, D.E. Sparks, B.H. Davis, Applied Catalysis a-General 269 (2004) 63.
[14] X.S. Liu, W. Ruettinger, X.M. Xu, R. Farrauto, Applied Catalysis B-Environmental 56 (2005) 69.
[15] S.L. Swartz, M.M. Seabaugh, C.T. Holt, W.J. Dawson, Fuel Cell Bull. 4 (2001) 7.
[16] R. Craciun, B. Shereck, R.J. Gorte, Catalysis Letters 51 (1998) 149.
[17] R. Farrauto, S. Hwang, L. Shore, W. Ruettinger, J. Lampert, T. Giroux, Y. Liu, O. Ilinich, Annual Review of Materials Research 33 (2003) 1.
[18] A. Bueno-Lopez, K. Krishna, M. Makkee, J.A. Moulijn, Journal of Catalysis 230 (2005) 237.
[19] R.M. Heck, R.J. Farrauto, Applied Catalysis a-General 221 (2001) 443.
[20] J. Kaspar, P. Fornasiero, in A. Trovarelli (Editor), Catalysis by Ceria and Related Materials, Imperial College Press; London, 2002.
[21] T. Kim, J.M. Vohs, R.J. Gorte, Industrial & Engineering Chemistry Research 45 (2006) 5561.
[22] P.R. Shah, T. Kim, G. Zhou, P. Fornasiero, R.J. Gorte, Chemistry of Materials 18 (2006) 5363.
[23] G. Zhou, P.R. Shah, T. Kim, P. Fornasiero, R.J. Gorte, Catalysis Today 123 (2007) 86.
[24] K. Eguchi, T. Setoguchi, T. Inoue, H. Arai, Solid State Ionics 52 (1992) 165.
[25] G. Zhou, P.R. Shah, T. Montini, P. Fornasiero, R.J. Gorte, Surface Science 601 (2007) 2512.
[26] D.A. Andersson, S.I. Simak, N.V. Skorodumova, I.A. Abrikosov, B. Johansson, Applied Physics Letters 90 (2007) 031909.
[27] G. Dutta, U.V. Waghmare, T. Baidya, M.S. Hegde, K.R. Priolkar, P.R. Sarode, Chem. Mater. 18 (2006) 3249.
[28] S. Yang, W. Zhu, Z. Jiang, Z. Chen, J. Wang, Applied Surface Science 252 (2006) 8499.

[29] J. Rynkowski, J. Farbotko, R. Touroude, L. Hilaire, Applied Catalysis A: General 203 (2000) 335.
[30] A.P. Hammersley, S.O. Svensson, A. Thompson, Nuclear Instruments and Methods in Physics Research Section A: Accelerators, Spectrometers, Detectors and Associated Equipment 346 (1994) 312.
[31] B.M. Reddy, A. Khan, P. Lakshmanan, M. Aouine, S. Loridant, J.C. Volta, J. Phys. Chem. B 109 (2005) 3355.
[32] D.A. Andersson, S.I. Simak, N.V. Skorodumova, I.A. Abrikosov, B. Johansson, To be published (2007).
[33] S. Kim, R. Merkle, J. Maier, Surface Science 549 (2004) 196.
[34] Y.M. Chiang, E.B. Lavik, D.A. Blom, Nanostructured Materials 9 (1997) 633.
[35] D.J.M. Bevan, J. Kordis, Journal of Inorganic & Nuclear Chemistry 26 (1964) 1509.
[36] D.R. Lide, CRC Handbook of Chemistry and Physics, CRC Press, Boca Raton, FL, 2005.
[37] M. Mogensen, N.M. Sammes, G.A. Tompsett, Solid State Ionics 129 (2000) 63.
[38] H. Otobe, A. Nakamura, T. Yamashita, K. Minato, Journal of Physics and Chemistry of Solids 66 (2005) 329.
[39] R.J. Gorte, Catalysis Today 28 (1996) 405.
[40] S. Zhao, R.J. Gorte, Catalysis Letters 92 (2004) 75.

Table 1

| Sample* | Lattice constant (Å) | Crystalline size (Å) | strain | Profile fit Rwp | Surface area ($m^2/g$) |
|---|---|---|---|---|---|
| CeO2 723 K | 5.4141 | 88 | - | - | 94 |
| CeO2 1173 K[a] | 5.4149 | 1086 | - | - | 2 |
| Ce9Ti1 973 K | 5.4029 | 82 | 0.37386 | 2.34% | 63 |
| Ce8Ti2 973 K | 5.4045 | 89 | 0.34009 | 2.30% | 60 |
| Ce9Ti1 1323 K | 5.4114 | 693 | 0.01613 | 4.86% | 0.2 |
| Ce8Ti2 1323 K | 5.4119 | 1086 | 0.01612 | 4.24% | 0.6 |

*The samples were calcined at 973 K for 5 hr and at 1323 K for 5 hr.

[a]The ceria data was obtained from our previous paper [23].

Table 2

| Sample* | Surface area ($m^2/g$) | Activation energy (kJ/mol) |
|---|---|---|
| 1wt%Pd/$CeO_2$ | 101 | 44 |
| 1wt%Pd/$Ce_{0.81}Zr_{0.19}O_2$ | 81 | 45 |
| 1wt%Pd/$Ce_{0.8}Ti_{0.2}O_2$ | 68 | 40 |

* Pd was added by wet impregnation, and samples were calcined at 723 K for 5 hr.

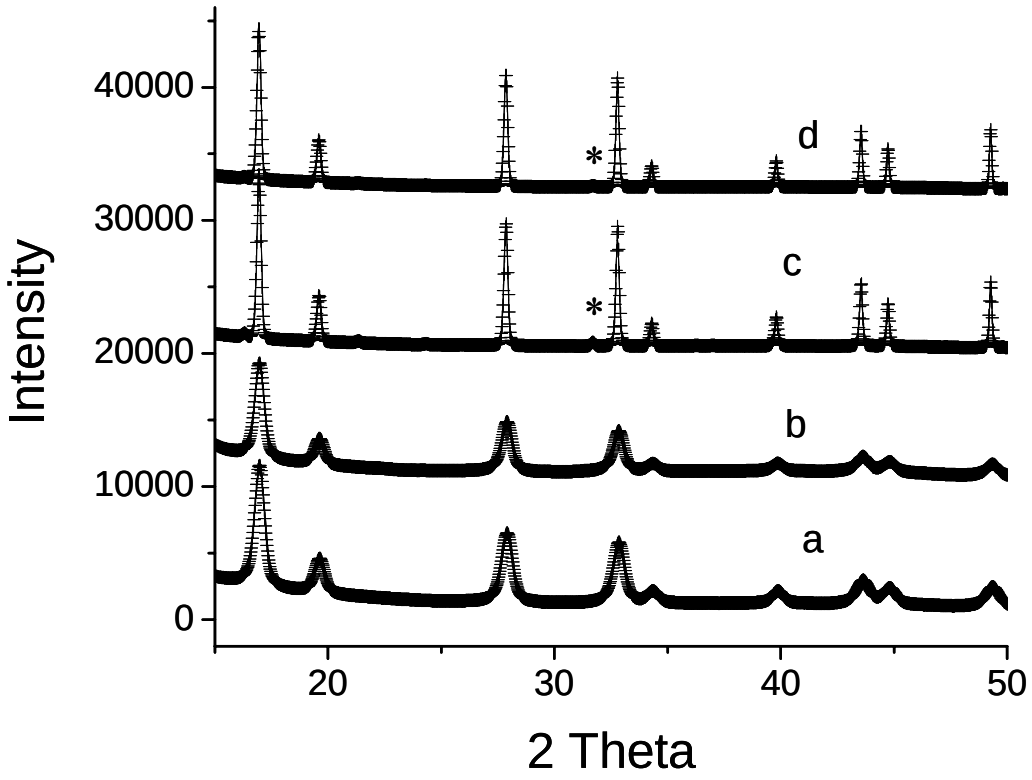


Figure 1. XRD patterns for ceria-titania mixed oxides: a) $Ce_{0.9}Ti_{0.1}O_2$ calcined at 973 K for 5 h, b) $Ce_{0.8}Ti_{0.2}O_2$ calcined at 973 K for 5 h, c) $Ce_{0.9}Ti_{0.1}O_2$ calcined at 1323 K for 5 h, and d) $Ce_{0.8}Ti_{0.2}O_2$ calcined at 1323 K for 5 h. The calculated profiles are solid lines and the experimental data are marked with + signs. The symbols (*) show the presence of weak rutile peaks on ceria-titania mixed oxides calcined at 1323 K.

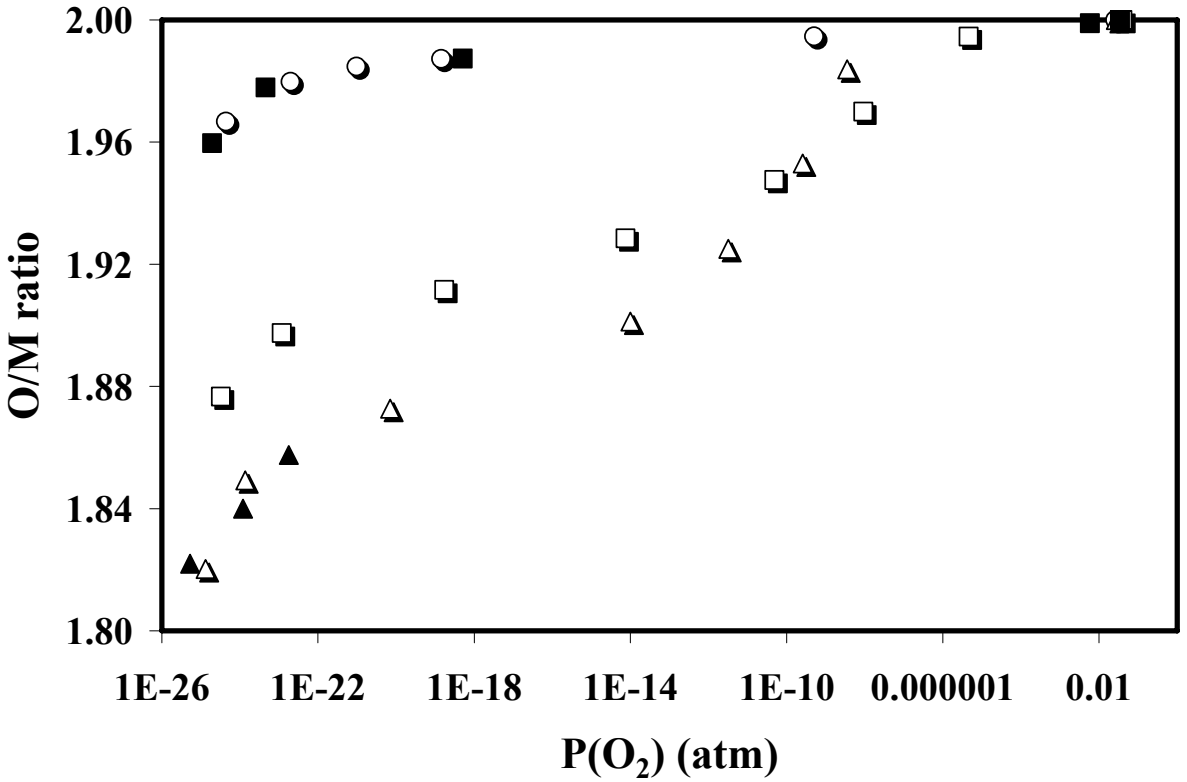


Figure 2. Oxygen-to-metal ratios for (○) $CeO_2$, (□) $Ce_{0.9}Ti_{0.1}O_2$, and (Δ)$Ce_{0.8}Ti_{0.2}O_2$ as a function of $P(O_2)$ at 973 K, measured by coulometric titration, for samples were calcined at 973 K for 5 hours. The closed squares (■) show oxygen-to-metal ratios for $Ce_{0.9}Ti_{0.1}O_2$ at 973 K after the sample had been calcined at 1323 K. The closed triangles (▲) show the oxygen to metal ratio of $Ce_{0.9}Ti_{0.1}O_2$ at 973 K measured using flow titration.

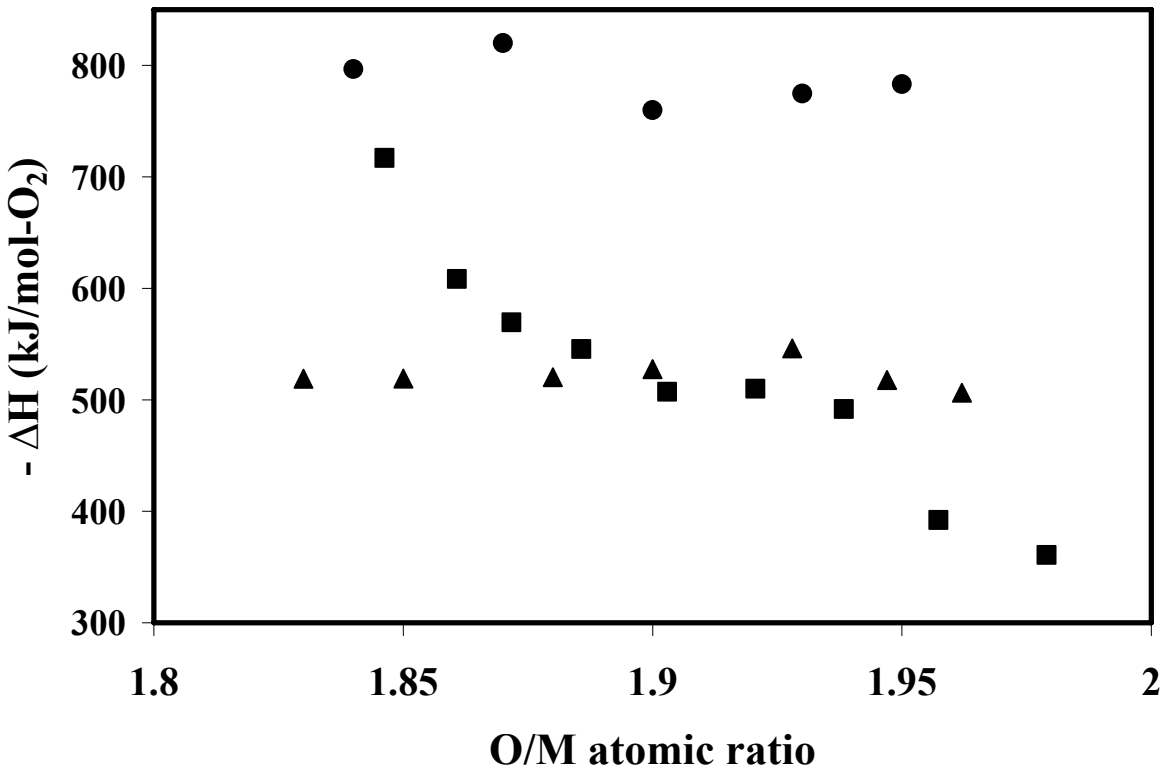


Figure 3. Oxidation enthalpies (-ΔH) for (■) $Ce_{0.8}Ti_{0.2}O_2$ , (▲) $Ce_{0.81}Zr_{0.19}O_2$ and (●) $CeO_2$ as a function of stoichiometry at 973 K.

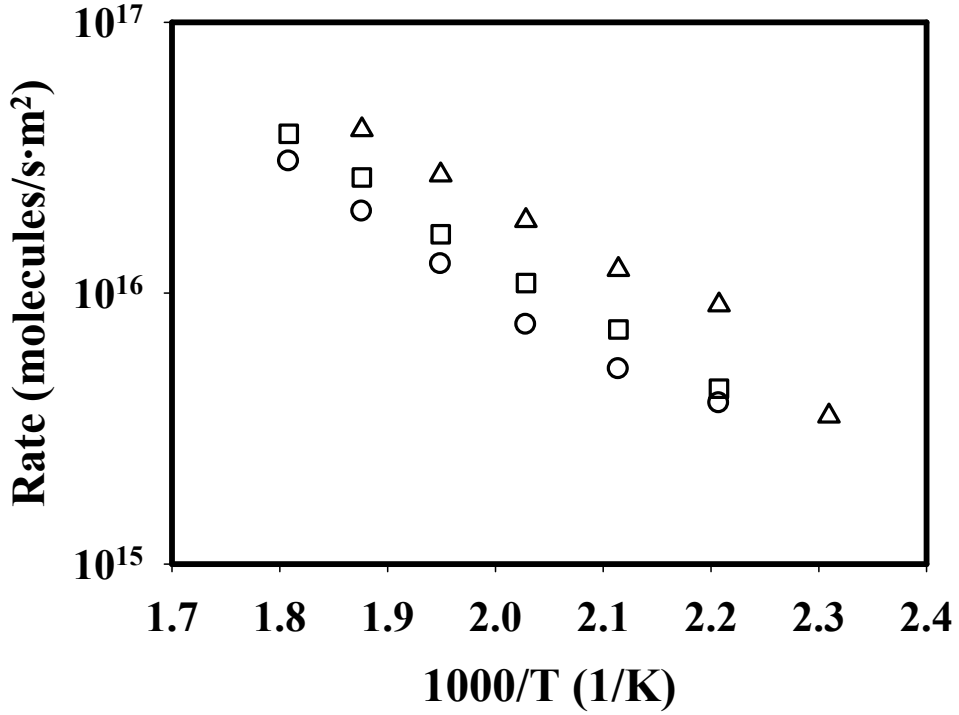


Figure 4. Differential reaction rates for the WGS reaction over (○) 1wt% $Pd/CeO_2$, (□) 1wt% $Pd/Ce_{0.81}Zr_{0.19}$, and (Δ)1wt% $Pd/Ce_{0.8}Ti_{0.2}O_2$.